Cardiolipin Switch in Mitochondria: Shutting off the Reduction of Cytochrome *c* and Turning on the Peroxidase Activity†

Liana V. Basova,‡ Igor V. Kurnikov,‡ Lei Wang,§ Vladimir B. Ritov,‡ Natalia A. Belikova,‡ Irina I. Vlasova,‡ Andy A. Pacheco,|| Daniel E. Winnica,‡ Jim Peterson,‡ Hülya Bayir,‡,⊥ David H. Waldeck,§ and Valerian E. Kagan*,‡

Center for Free Radical and Antioxidant Health, Department of Environmental and Occupational Health, Department of Chemistry, and Department of Critical Care Medicine, University of Pittsburgh, Pittsburgh, Pennsylvania 15260, and Department of Chemistry, University of Wisconsin—Milwaukee, Milwaukee, Wisconsin 53211

Received September 5, 2006; Revised Manuscript Received January 16, 2007

ABSTRACT: Upon interaction with anionic phospholipids, particularly mitochondria-specific cardiolipin (CL), cytochrome *c* (cyt *c*) loses its tertiary structure and its peroxidase activity dramatically increases. CL-induced peroxidase activity of cyt *c* has been found to be important for selective CL oxidation in cells undergoing programmed death. During apoptosis, the peroxidase activity and the fraction of CL-bound cyt *c* markedly increase, suggesting that CL may act as a switch to regulate cyt *c*'s mitochondrial functions. Using cyclic voltammetry and equilibrium redox titrations, we show that the redox potential of cyt *c* shifts negatively by 350−400 mV upon binding to CL-containing membranes. Consequently, functions of cyt *c* as an electron transporter and cyt *c* reduction by Complex III are strongly inhibited. Further, CL/cyt *c* complexes are not effective in scavenging superoxide anions and are not effectively reduced by ascorbate. Thus, both redox properties and functions of cyt *c* change upon interaction with CL in the mitochondrial membrane, diminishing cyt *c*'s electron donor/acceptor role and stimulating its peroxidase activity.

Cytochrome *c* (cyt *c*)[1] is a globular redox protein that shuttles electrons between respiratory Complexes III and IV in mitochondria (*1*, *2*). Despite almost 80 years of studies and a vast accumulation of data, new facets of its biological role have been discovered recently. One newly established function of cyt *c*, associated with its electron donor−acceptor properties, is realized during its interactions with superoxide (*3*). In this capacity, cyt *c* assumes an antioxidant role by effective quenching of this oxygen radical (*4*). Another newly discovered function of cyt *c*, which is not redox-related, is realized outside of mitochondria. After its release into the cytosol during apoptosis (*5*, *6*), cyt *c* binds to Apaf-1 protein, causing its oligomerization, and thus activates caspase cascades (*7*).

Recently, we described another important role of cyt *c* in apoptosis in which it displays peroxidase behavior (*8*). Cyt *c* acts as a catalyst for peroxidation of cardiolipin (CL), which is a mitochondria-specific anionic phospholipid, by hydrogen peroxide that is generated in the early stages of apoptosis. CL peroxidation contributes to the permeabilization of the outer mitochondrial membrane and the release of cyt *c* and other proapoptotic factors from the intermembrane space into the cytosol. At later stages of apoptosis, the cytosolic cyt *c* catalyzes peroxidation of another anionic phospholipid, phosphatidylserine (PS), in the plasma membrane. Thus, it plays a part in PS externalization and generates an "eat-me" signal for clearance of apoptotic cells by macrophages (*9*).

The involvement of cyt *c* in several intramitochondrial tasks suggests that a regulation mechanism exists to switch from the electron shuttling (or normal) function to the peroxidase (or apoptotic) function of the hemoprotein. Under "normal" conditions Complex III (cytochrome bc_1) located in the inner mitochondrial membrane reduces cyt *c*, while Complex IV (cytochrome *c* oxidase) oxidizes it (*1*). Cyt *c* accepts electrons from Complex III at a redox potential of about +250 mV vs SHE while it donates electrons to the Cu_A site in Complex IV at a redox potential of around +285 mV vs SHE (*10*). Any significant change of the redox potential of cyt *c* is likely to disrupt the electron transfer reactions and inhibit electron transport between the complexes. One potentially important distinction between the mitochondrial "electron shuttle" pool of cyt *c* and the mitochondrial "peroxidase" pool of cyt *c* is the association of the latter with CL (*8*, *11*). The CL associated cyt *c* has a redox potential, which is significantly more negative than the "native" form (vide infra). During apoptosis, the peroxidase activity and the fraction of CL-bound cyt *c* markedly increase. These findings suggest that CL acts as a switch to regulate cyt *c*'s mitochondrial functions; however, specific

† This work was supported by the NSF (CHE-0415457), NIH (HL 70755, HL 61411, U19 AI 068021), NIOSH (OH 008282), Human Frontier Science Program, and Pennsylvania Department of Health (SAP 4100027294, AHA 0535365N).

* Corresponding author: e-mail, kagan@pitt.edu; tel, (412) 624-9479; fax, (412) 624-9361.

‡ Department of Environmental and Occupational Health, University of Pittsburgh.

§ Department of Chemistry, University of Pittsburgh.

|| Department of Chemistry, University of Wisconsin—Milwaukee.

⊥ Department of Critical Care Medicine, University of Pittsburgh.

[1] Abbreviations: cyt *c*, cytochrome *c*; CL, cardiolipin; TOCL, 1,1′,2,2′-tetraoleoylcardiolipin; DOPC or PC, 1,2-dioleoyl-*sn*-glycero-3-phosphocholine; CV, cyclic voltammetry; SAM, self-assembled monolayer; SHE, standard hydrogen electrode.

10.1021/bi061854k CCC: $37.00
Published on Web 02/24/2007

mechanisms through which this key function is realized remain to be elucidated.

Because porphyrin and two axial ligands (His-18 and Met-80) of iron in cyt *c* prevent direct interaction of hydrogen peroxide with the catalytic metal site, native cyt *c* in solution is a poor peroxidase (*12*). In the presence of CL- (or PS-) containing liposomes, the peroxidase activity of cyt *c* increases by 2 orders of magnitude (*8*, *11*, *13*). Apparently, increased peroxidase activity of cyt *c* upon its interaction with anionic membranes is associated with destabilization of its tertiary structure (*14*−*16*). Although interactions of cyt *c* with negatively charged membranes have been examined in numerous studies (*17*−*21*), the findings relevant to the redox properties of cyt *c* bound to anionic lipid membranes are conflicting. Tollin et al. reported a positive shift of the redox potential of cyt *c* interacting with a CL-containing bilayer deposited on the surface of an electrode (*22*). Wang et al. demonstrated a small negative shift of the cyt *c* redox potential upon interaction with CL-containing lipid monolayers (*23*). Electrochemical studies on metal electrodes covered with anionic self-assembled monolayers (SAMs) reveal a significant negative shift of the cyt *c*'s redox potential (*24*, *25*).

The redox potential of cyt *c* is critical to understanding its role in normally functioning mitochondria vs "death machines" in apoptotic cells. Therefore, in this work we examined the redox properties of cyt *c* in its complex with CL. The redox behavior of cyt *c* bound to anionic membranes was studied using two different approaches: direct electrochemistry of cyt *c* molecules bound to monolayers and redox titrations of cyt *c* bound to CL-containing liposomes. In addition, the effect of CL binding on the redox reactions of cyt *c* with isolated mitochondrial Complexes III and IV, as well as liver and brain mitochondria, and on the regulation of electron transport activity in the mitochondrial respirtatory chain was examined by an electron spin resonance technique (EPR) and optical absorbance. The data show that binding of cyt *c* to CL causes (1) a significant (∼350−400 mV) negative shift of the redox potential of cyt *c*, (2) an inhibition of cyt *c* reduction by purified respiratory Complex III and in mitochondria, (3) an interruption of mitochondrial electron transport, and (4) an inability to oxidize superoxide and ascorbate.

EXPERIMENTAL PROCEDURES

Materials. Horse heart cyt *c* (type C-7752, purity >95%), ascorbate, sodium hydrosulfite (dithionite, purity 87.7%), monobasic and dibasic sodium phosphate, HEPES, diethylenetriaminepentaacetic acid (DTPA), phosphate-buffered saline (PBS), hydrogen peroxide (H_2O_2), ethylene glycol bis-(2-aminoethyl ether)-*N*,*N*,*N*′,*N*′-tetraacetic acid (EGTA), sucrose, Tris, 2-methyl-2-nitrosopropane (MNP), myxothiazol, alamethicin, mannitol, xanthine, xanthine oxidase, 7-carboxy-1-heptanethiol [$HOOC-(CH_2)_7-HS$], and 1-cyclohexyl-3-(2-morpholinoethyl)carbodiimide metho-*p*-toluenesulfonate [$C_{14}H_{26}N_{30}C_7H_7O_3S$−carbodiimide linker (CMC)] were purchased from Sigma. Sodium lauryl maltoside (*n*-dodecyl β-D-maltopyranoside) was obtained from Anatrace Inc. 1,2-Dioleoyl-*sn*-glycero-3-phosphocholine (PC, DOPC) and 1,1′,2,2′-tetraoleoylcardiolipin (CL, TOCL) were purchased from Avanti Polar Lipids Inc.

Small unilamellar liposomes were prepared using a tip sonicator (Ultrasonic, Homogenizer 4710 Series; Cole-Palmer-Instrument Co., Chicago, IL) as described on the website www.avantilipids.com. Liposomes were made from TOCL and DOPC (1:1 molar ratio) and DOPC alone in 20 mM sodium phosphate or HEPES buffers containing 100 μM DTPA, pH 7.4.

Under conditions of our experiments, TOCL did not undergo autoxidation or any significant oxidation by the peroxidase activity of the cyt *c*/TOCL complex, as was verified by assessments of CL-OOH content using a sensitive fluorescence HPLC-based protocol (*8*). Indeed, even after 60 min incubation of TOCL (100 μM) in the presence of cyt *c* (4 μM) and H_2O_2 (100 μM) the contents of CL-OOH in the samples were very low and not significantly different from the controls (at 0 min incubation) (9.0 ± 1.0 vs 6.0 ± 0.6 pmol of CL-COOH/nmol of CL, respectively). In contrast, polyunsaturated tetralinoleoyl-CL (TLCL) was readily oxidized by the peroxidase activity of cyt *c*/CL: from 8.0 ± 0.9 to 160 ± 17.0 pmol of CL-OOH/nmol of CL (*26*). These results are in line with our previous report on high oxidizability of polyunsaturated CLs (such as TLCL or bovine heart CL) and the insensitivity of TOCL to oxidation catalyzed by the peroxidase activity of cyt *c*/CL complexes (*26*). Very low content of lipid peroxides in TOCL samples was also confirmed by EPR experiments that revealed no $g = 4.3$ EPR signals (indicating heme oxidation) from the mixture of cyt *c* and TOCL in the absence of exogenous H_2O_2 in the incubation system. However, the $g = 4.3$ EPR signal was readily detectable upon the addition of hydrogen peroxide.

Cyclic voltammetry (CV) was performed using a CH Instrument electrochemical analyzer 618B. The three-electrode electrochemical cell, which was used for collecting immobilized cyt *c* data, contained a platinum wire counter electrode, an Ag/AgCl (1 M KCl) reference electrode, and a SAM-modified gold working electrode. The Ag/AgCl reference electrode was calibrated against a saturated calomel electrode before experimentation. All redox potentials in this paper are reported versus the standard hydrogen electrode (SHE).

Electrode Preparation. A gold wire (0.5 mm diameter, purity 99.99%) was cleaned by reflux in concentrated nitric acid (68−70%) at 130 °C for 1 h and then was washed with deionized water. The tip of the gold wire was heated to form a ball of ∼0.06−0.15 cm^2 surface area. The gold ball was reheated in the flame until glowing and then quenched in deionized water. This annealing process was performed more than 15 times to make a smooth gold ball. The exposed gold wire was sealed in a glass capillary tube, and the gold ball tip was annealed and cooled in a high-purity stream of Ar gas.

Self-Assembled Monolayer (SAM) Solutions. For the pure carboxylic acid-terminated SAMs, the concentration of the solution was 2 mM alkanethiol in absolute ethanol. For the mixed carboxylic acid-terminated and hydroxyl-terminated alkanethiol (seven methylenes) SAMs, the total concentration of the solution was 2 mM at a ratio of 1:1.

Immobilization of Cyt c. Chemically modified electrodes were prepared by placing gold ball electrodes into the SAM solution overnight. Subsequently, the electrodes were removed from the solution, first rinsed with absolute ethanol,

then rinsed with the supporting buffer solution (10 mM sodium phosphate buffer, pH 7.0), and finally dried in a stream of dry argon gas. To immobilize cyt *c* covalently, the modified electrodes were placed into a 5 mM CMC solution in 100 mM sodium phosphate buffer at pH 7.0 for 0.5 h to activate the carboxyl group in the SAM. After the activation, the electrodes were rinsed with supporting buffer solution again and placed into 100 μM cyt *c* solution in 10 mM phosphate buffer at pH 7.0 for 1 h. To immobilize cyt *c* electrostatically, we skipped the carboxyl group activation step and directly placed the modified electrodes into the cyt *c* solution. After being rinsed with buffer solution, these electrodes were immediately used in voltammetry studies.

Redox Titration. The absorbance spectra of cyt *c* at different dithionite concentrations were recorded on a Cary Bio 50 UV/vis spectrophotometer. All dithionite titrations were performed in a glovebox under strictly anaerobic conditions. Two redox dyes (mediators) were used in the titration experiments: gallocyanine ($E^0 = +20$ mV) (*27*) and indigo carmine ($E^0 = -125$ mV). Concentrations of the reduced and oxidized forms of cyt *c* and mediators were obtained by least-squares fitting of the optical absorption spectra of the reaction mixture to a superposition of the individual optical spectra of the redox forms of the dyes, the liposomes, and the redox states of cyt *c* bound to liposomes at low and high lipid/protein ratios.

Isolation of Mitochondria. Liver mitochondria were isolated from male Sprague-Dawley rats using a Percoll gradient as described previously (*8*). The final pellet was frozen at −80 °C for later use.

Complex III Enzymatic Activity. Ubiquinol:ferricytochrome *c* oxidoreductase (Complex III) activity was measured in the absence of detergent by a modification of the method by Gudz et al. (*28*). Reduction of cyt *c* by decylubiquinol was monitored by an increase in the absorbance at 550 nm at 30 °C. To provide access of cyt *c* to Complex III, a mitochondria suspension [in 0.32 M sucrose in 10 mM Tris buffer (pH 7.4)] was subjected to nitrogen cavitation. The activity of Complex III was calculated from the difference between the rate of reduction of cyt *c* in the absence and in the presence of 2.5 μM specific Complex III inhibitor, myxothiazol (*29*). Decylubiquinol was prepared according to the method of Birch-Machin et al. (*30*).

Succinate-oxidase activity in mitochondria was measured after treatment with alamethicin using the assay of the fumarase dehydrogenase reaction to oxidize fumarate in the presence of cyt *c* (10 μM) and TOCL (62 μM)/DOPC (125 μM) and DOPC (250 μM) liposomes. The incubation medium contained KCN (*31*).

Complex III and IV Purification and Manipulations. Bovine Complexes III and IV were each purified from mitochondria isolated from beef hearts obtained from a local slaughter house. Complex III was subsequently isolated using a modified method of Hatefi as described by Ragan et al. (*32*). Complex IV was first separated from the mitochondrial preparations using a sodium cholate extraction and ammonium acetate precipitation as described by Ragan et al. and then finally purified by the ammonium sulfate/cholate procedure of Yonetani (*33*). Enzyme preparations were stored in liquid nitrogen (77 K) until used. The activity of enzymes (22 °C) was determined by spectrophotometric monitoring of cyt *c* reduction at 550 nm. Typically, the specific activity of Complex III preparations was 70−120 μmol min^{-1} mg^{-1}, and the turnover number of Complex IV preparations was 340 (±30)/s.

EPR Measurements. EPR spectra were recorded at room temperature on a JEOL-REIX spectrometer with 100 kHz modulation (Kyoto, Japan). A 50 μL sample was placed in Teflon tubing (0.8 mm internal diameter, 0.013 mm thickness) obtained from Alpha Wire Corp. (Elizabeth, NJ). The tubing was folded and placed in an open 3.0 mm internal diameter EPR quartz tube. EPR spectra of a reduced spin trap, MNP (MNP−H$^\bullet$, *tert*-butyl hydronitroxide), were recorded as follows: 3350 G, center field; 100 G, sweep width; 20 mW, microwave power; 0.79 G, field modulation; 4×10^3, receiver gain; 0.1 s, time constant; 4 min, scan time. The spectra of MNP−H$^\bullet$ are presented as an average of three recordings. The simulated spectra were generated using the WinSim program of the NIEHS public EPR software package (http://EPR.niehs.nih.gov). The ascorbate radical EPR spectra were recorded under the following instrumental settings: 3350 G, center field; 10 G, sweep width; 10 mW, microwave power; 0.5 G, field modulation; 10^3, receiver gain; 0.03 s, time constant; 4 min, scan time. The time courses of ascorbate radical generation were obtained by repeated scanning of the EPR spectrum (5 G, sweep width; other instrumental conditions were the same as above).

Cyt c Reduction by Ascorbate and Superoxide. The time course of cyt *c* reduction by ascorbate and superoxide generated in the xanthine/xanthine oxidase system (*34*) was recorded on a UV160U spectrophotometer (Shimadzu, Japan) in a 1.0 cm path length cuvette. For both reactions, cyt *c* was preincubated (15 min) with TOCL/DOPC (1:1) liposomes. Ascorbate or xanthine was added to start the reaction, and the absorbance at 550 nm was recorded for 10 and 5 min, respectively. The reference cuvette contained the same amount of liposomes.

Statistics. Data are expressed as means (SD) of at least triplicate determinations. Changes in variables were analyzed by one-way ANOVA for multiple comparisons. Difference was considered significant at $p < 0.05$.

RESULTS

Cyclic Voltammetry of Cyt c in the Presence of CL. Cyclic voltammetry was used to characterize the redox properties of CL/cyt *c* complexes. Cyt *c* molecules were covalently attached to the terminal carboxyl functionalities of alkanethiol (seven methylenes) SAM-coated gold electrodes. A typical cyclic voltammogram showed the reduction and oxidation peaks centered close to +220 mV (Figure 1a). Thus, the redox potential of cyt *c* on the anionic SAM is shifted by −40 mV vs that of cyt *c* in solution (+260 mV) (*35*). This shift is consistent with that reported earlier (*25*) and probably arises from the electrostatic field of negatively charged carboxylic groups of the SAM. Figure 1a shows the time-dependent changes of cyclic voltammograms of cyt *c* in the presence of TOCL liposomes. Addition of CL-containing liposomes (TOCL/DOPC, 1:1) resulted in a gradual disappearance of the reduction peak around +220 mV and the emergence of a new reduction peak around −200 mV, over the course of 1 h (Figure 1a). The oxidation peak was also shifted to more negative potentials, however only by about

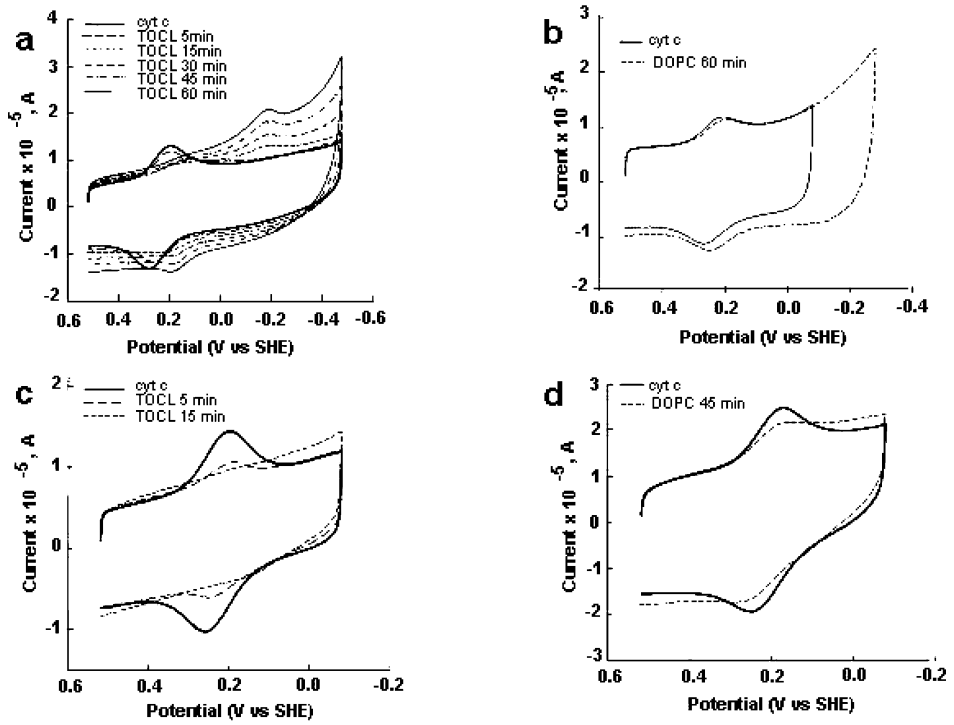

FIGURE 1: Cyclic voltammograms for cyt *c* covalently (a, b) and electrostatically (c, d) attached to carboxylic acid-terminated SAM covered gold electrodes in the presence of liposomes: 4 mM TOCL/DOPC (1:1) (a, c) and 4 mM DOPC alone (b, d). (a) Changes of the voltammograms of cyt *c* in the presence of TOCL liposomes were measured every 15 min during 60 min; (b) cyt *c* in the presence of DOPC after incubation during 60 min; (c) cyt *c* after incubation in TOCL liposomes during 5 and 15 min; (d) cyt *c* in the presence DOPC after incubation during 45 min. The voltammograms of cyt *c* without liposomes (solid line) are shown for comparison on each figure. Measurements were performed in 10 mM phosphate buffer at pH 7.0 and a scan rate of 20 V/s.

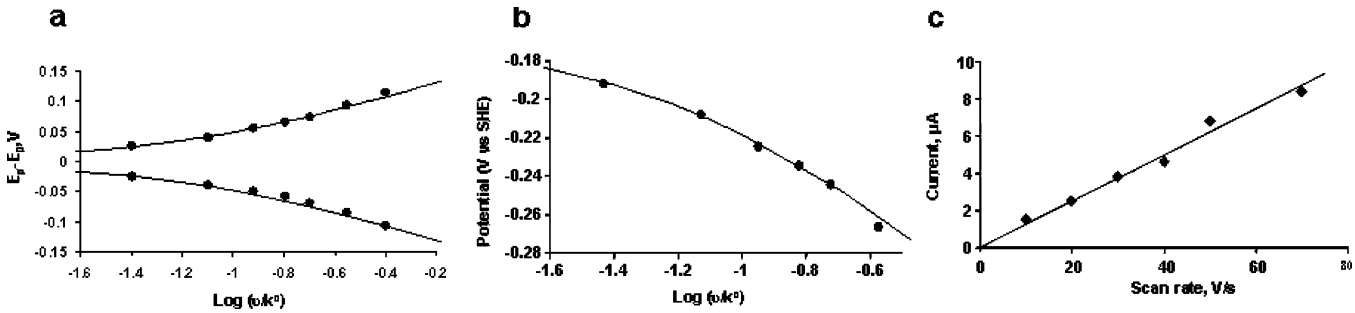

FIGURE 2: Scan rate dependence for cyt *c* in the absence (a) and in the presence of TOCL (b). Dependence of the reduction current upon the scan rate for the cyt *c*/TOCL complex is shown as well (c). Fits of the data to Marcus theory predictions are also shown for two different reorganization energies. See text for details.

50 mV. The appearance of the new reduction peak is consistent with the previously reported significant negative shift of the cyt *c*'s redox potential after its immobilization on SAMs containing puridine, imidazole, and nitrile functionalities that ligate axially to the heme moiety (*36*). More recently, Fedurco et al. (*37*) have detected new peaks (at ca. −200 mV) after denaturing of cyt *c* by 9 M urea. The very large separation (>300 mV) between reduction and oxidation peaks indicates a change in coordination of the Fe center. Apparently, TOCL interacts with cyt *c* and causes a change in the cyt *c* redox potential. In summary, the oxidized cyt *c* unfolds because of interactions with CL, regains its native conformation upon its reduction (at low electrode potentials), and loses its stability again upon oxidation (at high electrode potentials). Addition of pure DOPC liposomes did not result in changes of the position of either reduction or oxidation peaks of cyt *c*; however, the capacitive current increased (Figure 1b).

Cyt *c*, noncovalently (i.e., electrostatically) adsorbed on the carboxy-SAMs, also showed a disappearance of the reduction and oxidation peaks at +220 mV (Figure 1c, broken lines); however, no current was observed at negative potentials, likely because of desorption of the noncovalently attached TOCL/cyt *c* complexes from the electrode surface. The DOPC liposomes did not affect the redox peak positions of electrostatically attached cyt *c* (Figure 1d).

If the reduction wave is assumed to be reversible, the dependence of the peak position on the voltage scan rate can be used to find a standard electrochemical rate constant k^0 [this rate constant corresponds to $\Delta G = 0$ (*38*, *39*)]. For native cyt *c* the best fit based on Marcus theory of electron transfer gives a reorganization energy of 0.6 eV and a rate constant (k^0) of 250 s^{-1} (Figure 2a), which is in good agreement with previous works (*38*, *40*). Figure 2b shows a plot of the reduction peak shift versus the logarithm of the voltage scan rate for the TOCL/cyt *c* complex. The solid

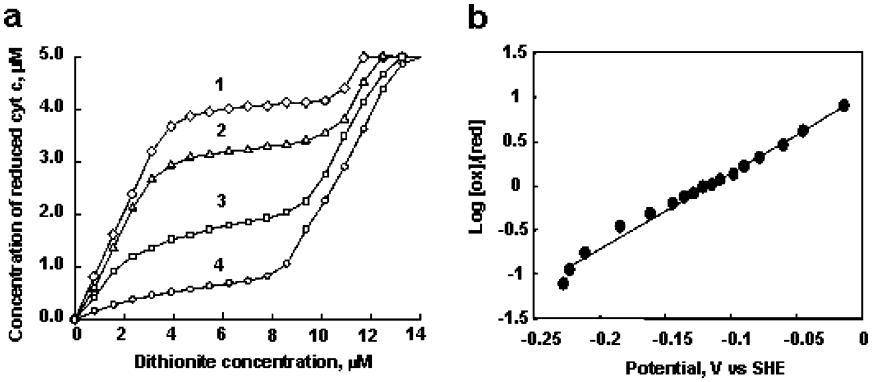

FIGURE 3: Redox titration of cyt *c* in the presence of TOCL by dithionite. (a) Concentration dependence of the reduced form of cyt *c* in the presence of TOCL and dithionite obtained by titration in the presence of gallocyanine (8 μM). The molar ratios of TOCL:cyt *c* were 25:1 (curve 1), 50:1 (curve 2), 100:1 (curve 3), and 200:1 (curve 4). (b) Nernst plot obtained from spectroelectrochemical titration of cyt *c* (5 μM) in complex with TOCL at the molar ratio of 1:200 versus the potential range of indigo carmine (10 μM). Cyt *c* was incubated with liposomes for 15 min, and then a redox mediator was added. After this, titration by dithionite was started. 2 μL of stock solution of fresh dithionite (0.8 μM) was added 20 times; after each addition the absorbance spectra from 700 to 250 nm were measured. Each point represents addition of dithionite. Gallocyanine and indigo carmine were used as indicators of the redox potential.

curve shows the best fit to the classical Marcus theory for the electron transfer rate constant. For the denatured form of cyt *c*, the best fit reorganization energy was 1.0 eV, and the rate constant k^0 was 270 s^{-1}, consistent with a higher mobility (closer approach to the electrode surface) and higher solvent accessibility of the heme of the denatured protein. At the scan rate of 10 V/s, the reduction peak potential was observed at −192 mV, and the characteristic potential for the reduction wave (E^0_r) was extrapolated to be −168 mV at 0 V/s. Unless one can reach high overpotentials, this method is not very sensitive to variations in the reorganization energy. The reduction currents associated with the denatured form of cyt *c* increased linearly with the scan rate (Figure 2c). This suggests that the current was limited by the electron transfer rate between the TOCL/cyt *c* complex and the electrode, and conformational transitions between denatured and native-like cyt *c* conformations proceeded on a faster time scale than electrode potential changes (scan rates 10−70 V/s) that cause these transitions ($>\sim 50$ s^{-1}). On the basis of the slope of the line, the surface concentration of the electroactive TOCL/cyt *c* complex was determined as 1.3 pmol/cm^2.

Redox Titration of Cyt c in the Presence of CL-Containing Liposomes. Although several research groups have studied the interaction of cyt *c* with different anionic phospholipids in liposomes (*11*, *13*−*23*), the redox properties of cyt *c* in the presence of CL-containing liposomes have not been characterized. The redox behavior of cyt *c* under equilibrium conditions was determined by titrating it with sodium dithionite ($E^0 = -564$ mV) (*41*) under anaerobic conditions and in the presence of indicator dyes (mediators) so that it could be followed optically. The cyt *c* in complex with CL-containing liposomes was titrated in the presence of gallocyanine redox dye. The standard redox potential of gallocyanine is +20 mV; thus at redox potentials higher than ∼+100 mV this dye is predominantly the oxidized form while at redox potentials lower than −100 mV it is predominantly the reduced form. Figure 3a shows the titration results for different molar ratios of TOCL/cyt *c*, ranging from 25:1 to 200:1 at pH 7.0. For low concentrations of TOCL (TOCL/cyt *c*, 25:1, 50:1), addition of dithionite reduced cyt *c* stoichiometrically while gallocyanine remained oxidized. After the addition of a certain amount of dithionite titrant, however, the reduction of cyt *c* almost completely stopped and did not resume until all of the gallocyanine was reduced. The titration results clearly showed the presence of two fractions of cyt *c* complexes. One fraction was reduced before the gallocyanine was reduced, thus it has a relatively high redox potential (>+100 mV), while the other fraction was reduced after the gallocyanine was reduced so that it must have a more negative redox potential (<−100 mV). Analysis of these titration curves shows that the fraction of cyt *c* with negative redox potential constitutes only about 20% of cyt *c* molecules at 25:1 CL/cyt *c* ratio but that this fraction increases to more than 90% at 200:1 TOCL/cyt *c* ratio. Our previous studies demonstrated that increasing the TOCL/cyt *c* ratios was associated with increased CL binding and denaturing of cyt *c* (*11*). Hence, it is likely that the easily reduced fraction of cyt *c* corresponds to protein molecules in a native-like conformation, whereas the fraction of cyt *c* with more negative redox potential corresponds to molecules partially denatured by the interaction with CL-containing liposomes.

To further characterize the redox properties of the cyt *c* that is denatured by CL, we performed dithionite titration of cyt *c* bound to TOCL/DOPC liposomes (200:1 lipids/protein ratio) in the presence of another redox mediator, indigo carmine. Figure 3b shows that cyt *c* bound to TOCL was gradually reduced as the redox potential changed from −20 to −220 mV (computed from the molar ratios of the reduced and oxidized indigo carmine species). The dependence of log([cyt c_{ox}]/[cyt c_{red}]) vs redox potential (Nernst plot) is approximately linear over the range of the redox potentials probed; however, the slope of the linear fit multiplied by 59 mV is 0.5 (±0.07), which differs substantially from the theoretical value of 1 that is expected from the Nernst equation for an one-electron process. The unusually small value of the slope of the Nernst plot and a wide range (∼200 mV) of redox potentials, over which the reduction of the membrane-bound cyt *c* occurs, indicates the presence of two or more subfractions in the low redox potential (denatured) fraction of cyt *c* bound to TOCL/DOPC liposomes. These data are in line with other reports that describe several subfractions of the denatured cyt *c*, which differ in heme ligation (*18*).

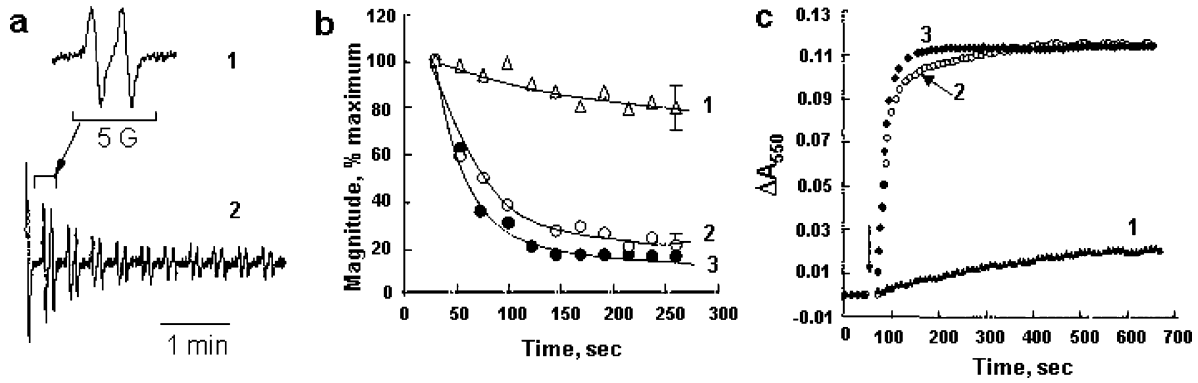

FIGURE 4: Effect of TOCL on cyt *c* reduction by ascorbate. (a) EPR spectrum (1) and time course (2) of ascorbate radicals formed in the incubation medium containing cyt *c* and ascorbate (25 μM cyt *c*, 500 μM ascorbate, 20 mM phosphate, and 100 μM DTPA, pH 7.4). (b) Time course of ascorbate radical generation in the absence (curve 3) or presence (curves 1 and 2) of liposomes. Cyt *c* (25 μM) was incubated with DOPC or TOCL/DOPC liposomes (1 mM) for 5 min at 21 °C, then ascorbate (500 μM) was added, and recording of the EPR ascorbate radical signal was started in 30 s. Results are normalized to the initial ascorbate radical signal intensity taken as 100%. (c) Time course of cyt *c* reduction by ascorbate in the presence and absence of TOCL/DOPC (1:1) and DOPC liposomes monitored by absorbance at 550 nm. Cyt *c* (5 μM; buffer, 20 mM HEPES and 100 μM DTPA) was preincubated with TOCL/DOPC (1:1) (100 μM) for 15 min at room temperature, then ascorbate (100 μM) was added, and absorbance was measured during 10 min (curve 1). Cyt *c* at the same concentration in the presence of ascorbate (curve 3) and DOPC (400 μM) liposomes (curve 2) is shown for comparison. The arrow indicates the time point when ascorbate was added.

We observed no detectable bleaching of the Soret band and no oxidation of reduced cyt *c* in the complex with CL for several hours of incubation of cyt *c* with TOCL/DOPC liposomes, indicating a very low content of peroxides in the lipid samples used.

Reduction of Cyt c/CL Complexes by Ascorbate. Ascorbate is a universal reductant in cells (*42*) and biofluids; the redox potential of ascorbate is +58 mV (*41*), i.e., significantly lower than that of cyt *c* (+260 mV) (*35*, *43*). Accordingly, ascorbate readily reduces cyt *c*. If the redox potential of TOCL/cyt *c* complexes is around −120 mV (50% reduction in redox titration experiments), it is unlikely that ascorbate can reduce the CL/cyt *c* complex. The reduction of cyt *c* in complex with TOCL by ascorbate was studied using two protocols: (1) we followed the one-electron reduction of ascorbate by the formation of its radical using EPR spectroscopy, and (2) we monitored cyt *c* reduction directly by its optical spectra. The typical doublet signal of the ascorbate radical with a hyperfine splitting constant of 1.7 G was detected upon incubation of ferri-cyt *c* with ascorbate (Figure 4a, curve 1). The time course of the ascorbate oxidation was observed as a rapid decrease of the ascorbate radical signal (Figure 4a, curve 2; Figure 4b, curve 3). In contrast, TOCL/cyt *c* complexes (20:1 molar ratio) oxidized ascorbate much less effectively (Figure 4b, curve 1). The slowing of the ascorbate oxidation rate by cyt *c* seems to be specific for TOCL, since the presence of DOPC liposomes did not inhibit the process (Figure 4b, curve 2). In line with these results, ascorbate reduction of cyt *c* alone and cyt *c* preincubated with PC was effective and rapid (Figure 4c, curves 2 and 3 accordingly), whereas TOCL/cyt *c* complexes displayed very slow reduction by ascorbate (Figure 4c, curve 1). The rate of reduction of cyt *c* in the presence of CL decreased 60 times as found by the comparison of initial slopes of reduction curves in Figure 4c. The decrease in the observed reduction rate due to the presence of CL corresponds to the change of the second-order rate constant for the reaction of ascorbate with cyt *c* from 2.1×10^5 M^{-1} s^{-1} (*43*) to 2.0×10^3 M^{-1} s^{-1}. Thus the reduction of cyt *c* bound to CL is effectively blocked, in agreement with the drastic negative shift of redox potential of the cyt *c* in the complex with CL.

We also monitored the reduction of cyt *c* in complex with CL by absorbance at 550 nm in anaerobic conditions. We found a slight increase in the rate of cyt *c* reduction (about 2 times at a CL/cyt *c* ratio of 20:1) as compared with our previous results in aerobic conditions, but it still remained 50 times lower than in the absence of CL. EPR measurements also demonstrated the similarity of time course of ascorbate radical formation in aerobic and anaerobic conditions.

Interactions of CL/Cyt c Complexes with Superoxide. Because the redox potential of the O_2/O_2^- couple is about −130 mV (*44*), i.e., comparable with that of TOCL/cyt *c* complexes (see above), it was important to test whether electron transfer is possible between superoxide and TOCL/cyt *c*. A superoxide-generating system, xanthine oxidase/xanthine, was used to assess the reduction of cyt *c* (*34*) and its complex with TOCL (Figure 5a). The data in Figure 5b show that TOCL inhibited the reduction of cyt *c* by superoxide at TOCL/cyt *c* ratios >25:1, however less effectively than cyt *c* reduction by ascorbate. The observed rate of cyt *c* reduction dropped 5 times in the presence of CL (estimated by the comparison of initial slopes of reduction curves in Figure 5a). This decrease in reduction efficiency corresponds to a decrease of the bimolecular rate constant for the reaction of the superoxide anion with cyt *c* from 2.1×10^5 M^{-1} s^{-1} (*45*) to 4.2×10^4 M^{-1} s^{-1}. CL was less effective at inhibiting cyt *c* reduction by superoxide than the reaction with ascorbate, consistent with the more negative potential of superoxide, compared to that of ascorbate.

Effects of CL on the Reduction of Cyt c by Complex III. The first step in the interaction of ferri-cyt *c* with the electron transport chain is its reduction by Complex III. Effects of CL on the reduction of cyt *c* by Complex III were characterized using a purified enzyme by measuring the reduction of ferri-cyt *c* by decylubiquinol (ubiquinol:ferri-cyt *c* oxidoreductase activity) (*46*) (Figure 6a). Complex III effectively reduced oxidized cyt *c* (186 ± 7 units min^{-1} $nmol^{-1}$, curve 1). In contrast, in the presence of CL, the reaction was very slow (7.8 ± 0.3 units min^{-1} $nmol^{-1}$,

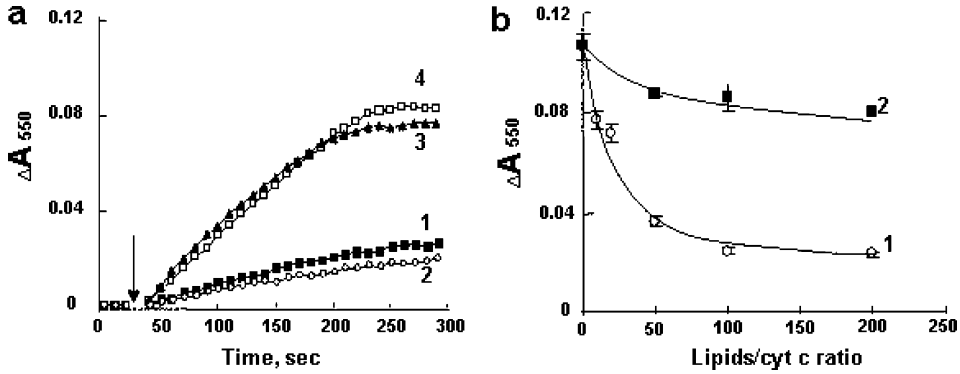

FIGURE 5: Cyt *c* reduction by superoxide radicals generated in the xanthine/xanthine oxidase system. (a) Time course of cyt *c* reduction by superoxide in the presence of TOCL/DOPC (curves 1 and 2) and DOPC (curve 3) liposomes and its absence (curve 4) monitored at 550 nm. Cyt *c* in the presence of DOPC (curve 3) and cyt *c* (curve 4) alone is shown for comparison. The arrow indicates the moment when xanthine oxidase was added. (b) Dependence of cyt *c* reduction by superoxide on lipid/cyt *c* ratio: TOCL/DOPC:cyt *c* (curve 1) and DOPC/cyt *c* (curve 2). Samples of cyt *c* (5 μM) were preincubated with TOCL/DOPC (1:1) liposomes at different concentrations for 15 min at room temperature in 20 mM HEPES buffer (plus 100 μM DTPA, pH 7.4). After the preincubation 25 μM xanthine (5 mM stock solution) was added, and the absorbance spectrum was recorded (the reference cuvette contained the same amount of liposomes). To start $O_2^{-\bullet}$ production xanthine oxidase was added (0.002 unit/mL). The time course of cyt *c* reduction was recorded every 10 s, measuring the absorption at 550 nm. After 5 min the total absorbance spectrum was recorded again. Differences between two spectra (ΔA_{550}) were calculated after alignment in the 530−570 nm region.

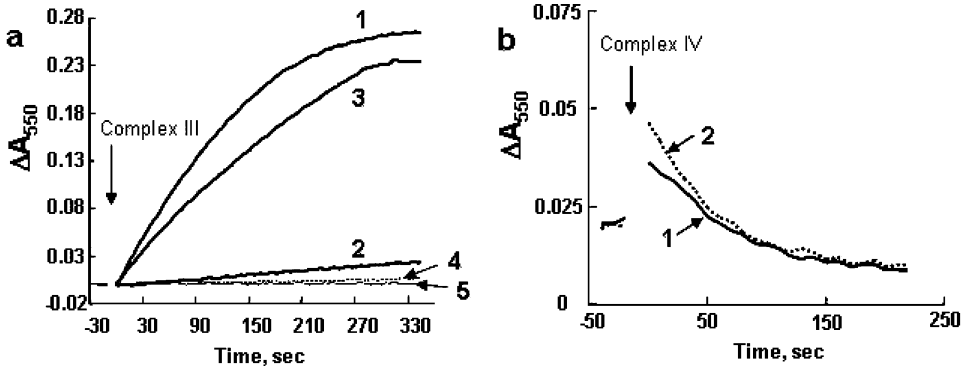

FIGURE 6: Effect of CL on the activities of purified Complexes III and IV. (a) Reduction of cyt *c* by Complex III in the absence (curve 1) and in the presence of TOCL/DOPC (curve 2) or DOPC liposomes (curve 3). Cyt *c* (25 μM) was preincubated for 15 min with liposomes (5 mM); then Complex III was added (10 nM). The incubation system was composed of 20 mM HEPES with 100 μM DTPA, lauryl maltoside (0.1%), and decylubiquinol (100 μM), pH 7.4. Control experiments showing the reduction of cyt *c* in the presence of (a) lauryl maltoside (0.1%) and decylubiquinol (100 μM) (curve 4) and lauryl maltoside (0.1%), decylubiquinol (100 μM), and myxothiazol (2.5 μM) (curve 5). The arrow indicates the addition of Complex III. (b) Oxidation of cyt *c* in the absence (curve 1) and in the presence (curve 2) of TOCL/DOPC liposomes by isolated Complex IV. The concentration of cyt *c* was 10 μM (alone) and 50 μM (in complex with TOCL); the concentration of Complex IV was 50 nM. Buffer contained 20 mM HEPES (pH 7.4) with 100 μM DTPA and lauryl maltoside (0.1%). Liposomes were preincubated with cyt *c* for 5 min. The arrow indicates the addition of Complex IV.

curve 2). The specificity of interactions of cardiolipin-bound cyt *c* with Complex III was confirmed by control experiments showing that (1) the reduction of cyt *c* by purified Complex III was completely inhibited in the presence of its specific inhibitor, myxothiazol (*29*) (curve 5), (2) the reduction of cyt *c* by decylubiquinol did not occur in the absence of Complex III (curve 4), and (3) DOPC liposomes did not significantly affect the reduction of cyt *c* by Complex III in the absence of cardiolipin (the rate of cyt *c* reduction was 130.6 ± 5.2, curve 3).

The effect of CL on the electron transfer between Complex III and cyt *c* was further assessed in the inner membrane of mitochondria, in the presence of either DOPC liposomes or a mixture of TOCL/DOPC (1:1) liposomes. For rat liver mitochondria, the rate of cyt *c* reduction by decylubiquinol decreased from 3.7 ± 0.2 to 2.6 ± 0.1 milliunits min^{-1} (mg of protein)$^{-1}$ in the presence of TOCL. Similarly, TOCL decreased the rate of cyt *c* reduction in rat brain cortex mitochondria from 2.6 ± 0.2 to 0.9 ± 0.1 milliunit min^{-1} (mg of protein)$^{-1}$ in the presence of TOCL. When the activity of cyt *c* reduction was determined in the presence of myxothiazol, the reaction was 12-fold slower than in the absence of the inhibitor (data not shown). Further, the Complex III-mediated reduction of cyt *c* by decylubiquinol was much less sensitive to DOPC-containing liposomes (lacking TOCL).

Effect of CL on Complex IV Activity. While the negative shift of cyt *c*'s redox potential upon binding CL precludes its reduction by Complex III, the reduced cyt *c* should remain a good donor of electrons for Complex IV. Indeed, purified Complex IV oxidized ferro-cyt *c* complexed with TOCL (Figure 6b, curve 2) as effectively as ferro-cyt *c* without CL (Figure 6b, curve 1). The cyt *c* oxidation rate was 6.6 ± 0.1 and 10.5 ± 0.14 units min^{-1} $nmol^{-1}$ in the absence and presence of TOCL liposomes, respectively. In line with this, exogenously added TOCL-containing liposomes had no effect on the activity of Complex IV in mitochondria (assessed in the presence of lauryl maltoside, 0.1%).

Inhibition of Mitochondrial Electron Transport by CL. To further test the hypothesis that cyt *c* in complex with CL

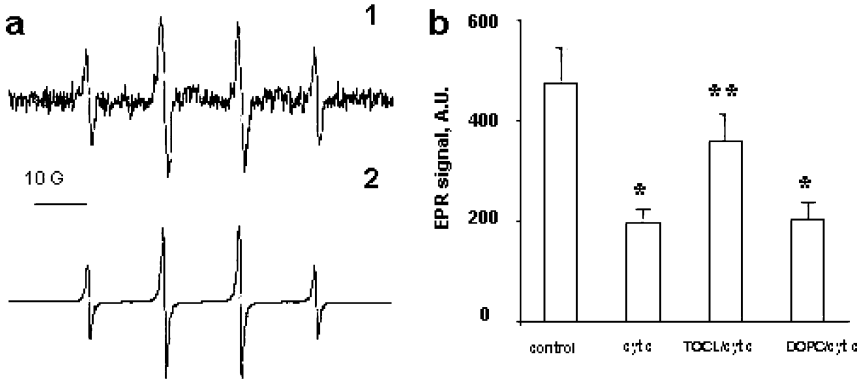

FIGURE 7: Effect of cyt *c* on the EPR signal of MNP reduced to MNP−H• in the rat liver mitochondrial suspension. The mitochondrial suspension (4 mg of protein/mL) in buffer (230 mM mannitol, 70 mM sucrose, 20 mM Tris-HCl, 2.5 mM phosphate, 0.5 mM EGTA, pH 7.4) was supplemented with 20 mM MNP and succinate (7.5 mM). Spectra of reduced MNP (MNP−H•) were recorded 10 min after succinate addition. (a) EPR spectrum of MNP−H•: 1, an experimental spectrum; 2, computer simulation using hyperfine coupling constants $a^N = a^H\beta = 14.4$ G. (b) Magnitude of the EPR signal of MNP−H•. Control: magnitude of the MNP−H• signal after addition of succinate to the mitochondrial suspension. Cyt *c* (20 μM) with or without liposomes (400 μM total lipid) was added to mitochondria before addition of succinate. The results are representative of five independent experiments. Data are presented as the mean ± SE ($n = 3$) (*, $p < 0.01$ vs control; **, $p < 0.05$ vs cyt *c*).

cannot operate as an effective electron shuttle in the mitochondrial respiratory chain, we studied the effects of exogenously added TOCL on succinate-dependent electron transport through respiratory complexes of mitochondria using two different approaches. In the first one, we examined succinate-dependent reduction of a spin trap, MNP, to MNP−H• (*47*). We employed mitochondria with their outer membrane mechanically removed by the nitrogen cavitation protocol. After addition of succinate to mitochondria incubated in the presence of MNP, a typical four-line EPR spectrum of the MNP−H• radical was observed (Figure 7a), in line with the known one-electron reduction of MNP by mitochondrial electron transport (*47*). Expectedly, the magnitude of the signal (concentration of MNP−H•) increased over 10 min (*48*, *49*). Thus, succinate-induced reduction of MNP occurred in the absence of endogenous cyt *c* washed away from the intermembrane space during the removal of the outer membrane (Figure 7b). Addition of exogenous cyt *c* resulted in a significant decrease of the signal intensity. Cyt *c* added along with TOCL/DOPC liposomes was much less efficient in quenching of the MNP−H• signal. Without TOCL, DOPC liposomes did not affect cyt *c* dependent quenching of the succinate-induced signal. These results demonstrate that the electron acceptor function of cyt *c* in mitochondria was impaired by CL.

In a separate series of experiments, we further tested effects of TOCL on succinate-dependent electron transport through respiratory complexes of liver and brain mouse mitochondria. Electron transport (succinate oxidase) activity in mitochondria was measured before and after treatment with alamethicin, which is known to permeabilize mitochondrial membranes and remove loosely (electrostatically) bound cyt *c* from mitochondria. Alamethicin caused almost complete inhibition of succinate oxidase activity and a removal of most (~85%) cyt *c* from mitochondria, in line with previously published results (*31*, *50*, *51*). For both liver and brain mitochondria, the electron transport activity could be fully restored by exogenously added cyt *c*. When TOCL/DOPC liposomes were added along with cyt *c*, however, the reconstitution of succinate oxidase activity was incomplete and dependent on the amount of TOCL such that at a TOCL/cyt *c* ratio of 20:1, only 25% of succinate oxidase activity could be reconstituted. DOPC had essentially no effect on the succinate oxidase activity. These results suggest that interaction of cyt *c* with CL inhibits cyt *c*'s ability to effectively participate in electron transport.

Cyclic Voltammetry of the Peroxidase Reaction Catalyzed by Cyt c in the Presence of CL. The peroxidase activity of cyt *c* and its dependence on CL was studied by cyclic voltammetry of cyt *c* electrostatically (Figure 8a) and covalently (Figure 8b,c) attached to SAM-covered gold electrodes. Addition of H_2O_2 resulted in a concentration-dependent decrease of magnitudes of +220 mV oxidation and reduction peaks and the appearance of reduction and oxidation peaks at about −200 mV potential (Figure 8a). A probable interpretation of these observations is that the chemical modification of cyt *c*, as a result of the peroxidase reaction, reduces the protein stability so that it is more vulnerable to denaturation by the anionic SAM. The position of the reduction wave for cyt *c* reacted with H_2O_2 was similar to the reduction wave of cyt *c* modified by the interaction with TOCL; however, the oxidation peak of cyt *c* reacted with H_2O_2 was observed at a potential of approximately −200 mV while TOCL/cyt *c* complexes were oxidized around +100 mV. Apparently, the reduction of chemically intact cyt *c* denatured by CL is accompanied by a conversion of cyt *c* into a native-like conformation, with respect to the heme pocket. In contrast, cyt *c* molecules chemically damaged by H_2O_2 are not refolded by heme reduction.

At higher H_2O_2 concentrations, a complete disappearance of the native cyt *c* redox waves was observed along with the appearance of H_2O_2 concentration-dependent reduction waves at the negative potentials (Figure 8b). Apparently, reactive compounds I and II of cyt *c*, formed as a result of the peroxidase reaction, were quickly reduced by neighboring reduced cyt *c* molecules. Consequently, the concentration of the oxidized (and denatured) forms of cyt *c* increased, resulting in greater amplitude of the reduction wave at the negative electric potentials. The peroxidase activity of cyt *c* in the presence of TOCL was higher than in its absence (compare the current in the negative potential region to the peak current of the reversible cyt *c* wave in panels c and b of Figure 8).

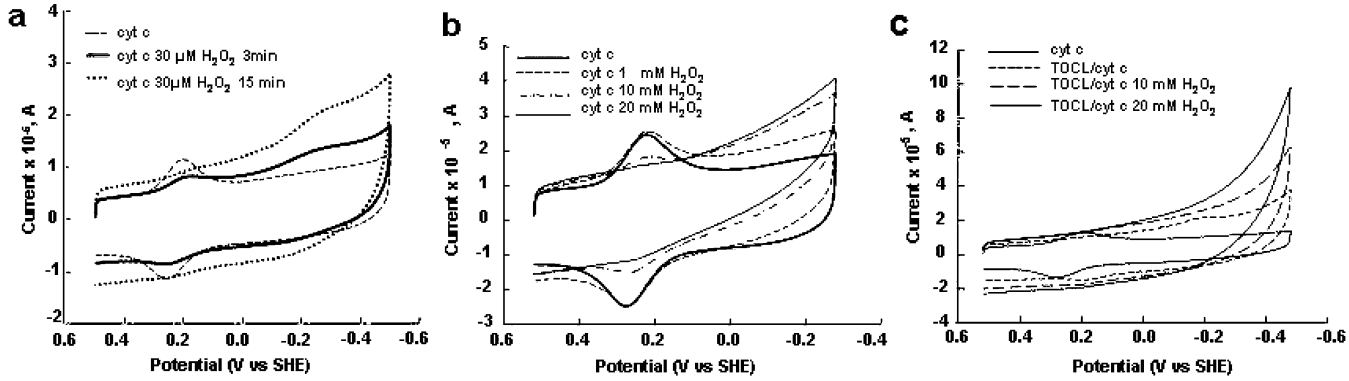

FIGURE 8: Cyclic voltammograms of cyt *c* electrostatically attached to carboxylic acid terminated in the absence (dashed line) and the presence of 30 μM H_2O_2 after 3 (solid line) and 15 (dotted line) min incubation with H_2O_2. (a) Cyclic voltammograms of cyt *c* covalently attached to SAM at different concentrations of H_2O_2 in the absence (b) and presence of TOCL/DOPC liposomes (c). Cyt *c* was incubated with liposomes during 60 min, and then H_2O_2 was added. The voltammograms were recorded after preincubation with H_2O_2 during 15 min under N_2. The voltammograms of cyt *c* without liposomes at pH 7.0 are shown for comparison on both figures (solid line). Scan rate = 20 V/s.

As the reduction current kept increasing while the electrode potential decreased, we were not able to find a "peak" or flattening of the reduction wave. However, we detected a flattening of the H_2O_2-sensitive reduction wave in analogous experiments with the MP-11 cyt *c* fragment (data not shown). Experiments showed that the reduction "wave" was not sensitive to the presence of oxygen. In the absence of cyt *c*, H_2O_2 alone did not produce a discernible electrochemical response in the potential range investigated.

DISCUSSION

CL as a Switch of Cyt c Peroxidase Activity. Our previous work has identified CL/cyt *c* complexes as important components of mitochondrial machinery that are triggered by proapoptotic stimuli and initiate the release of proapoptotic factors, including cyt *c* (*8*). This engages subsequent segments of the cell death program such as caspase cascades. The essential redox function of CL/cyt *c* complexes is realized through their specific peroxidase activity directed toward oxidation of polyunsaturated molecular species of CL and accumulation of CL oxidation products, which act as proapoptotic signals in mitochondria (*8*). The molecular switch that turns off the electron shuttling function of cyt *c* and turns on its peroxidase activity was not specifically identified, however. It is tempting to speculate that the same CL that binds cyt *c* and causes its partial unfolding acts as a switch playing this important role.

This work demonstrates that the redox potential of cyt *c* shifts negatively by about 350−400 mV upon its interaction with CL-containing phospholipid membranes. Redox titration experiments showed the simultaneous presence of two fractions of cyt *c* in the complex with CL: one readily reducible, with a native-like redox potential, and the second fraction, more resistant to reduction, with a more negative redox potential. The population of the protein fraction resistant to reduction grew with the increase in lipid/protein ratio and apparently corresponded to cyt *c* molecules unfolded by interactions with CL membranes, previously identified by tryptophan fluorescence measurements in similar conditions (*11*). The redox titration also showed that the reduction-resistant fraction of cyt *c* bound to CL (denatured cyt *c* molecules) was heterogeneous and consisted of two or more subfractions, reducible over a wide range of redox potentials between −50 and −200 mV. This finding is consistent with an analysis by Hildebrandt et al. (*18*), who showed that fractions of cyt *c* denatured on Ag electrodes with different ligation (in Hildebrandt's classification pentacoordinate B2/5cHS and hexacoordinate B2/6cLS) have different redox potentials (in the range of −93 and −143 mV, respectively).

Our control experiments that included monitoring of cyt *c* Soret band bleaching and EPR detection of the spin state of heme as well as protein-immobilized radical species (reactive intermediates) confirmed that no detectable peroxidase activity was displayed by the cyt *c*/CL complexes in the absence of exogenous peroxides. Therefore, the observed changes of the redox properties of cyt *c* in its complexes with CL are not associated with chemical damage of cyt *c*.

We established that CL prevents reduction of cyt *c* by Complex III, ascorbate, and superoxide and blocks its participation in mitochondrial electron transport. Experiments with purified Complexes III and IV strongly support our conclusion that the negative shift of the cyt *c* redox potential induced by CL rather than its physical separation from the mitochondrial complexes is the major mechanism to turn off the electron transporting function of cyt *c* in the mitochondrial respiratory chain. The inhibitory effects of CL were concentration-dependent, in agreement with our finding of two fractions of CL/cyt *c* with drastically different redox properties. Our assessments of ubiquinol:ferri-cyt *c* oxidoreductase showed that CL can compete with Complex III for cyt *c*. Therefore, operation of the electron transport chain in mitochondria appears to depend on the availability of CL (*2*). Normally, over 95% of CL is confined to the inner mitochondrial membrane (*8*). During apoptosis, CL migrates from the inner leaflet to the outer leaflet of the inner membrane and further to the outer mitochondrial membrane, setting the stage for its facilitated interaction with cyt *c*. Apoptosis-associated redistribution of CL between the inner and outer mitochondrial membranes (*52*) makes CL available for binding with cyt *c*, thus causing a negative shift of its redox potential and converting it into a peroxidase (*8*). Recent data show that CL plays a very important role in structural

Scheme 1: Interactions of Cyt *C* with CL Resulting in a Drastic Negative Shift of the Cyt *c* Redox Potential: A Possible Mechanism of Disruption of Mitochondrial Electron Transport and Increased Production of ROS

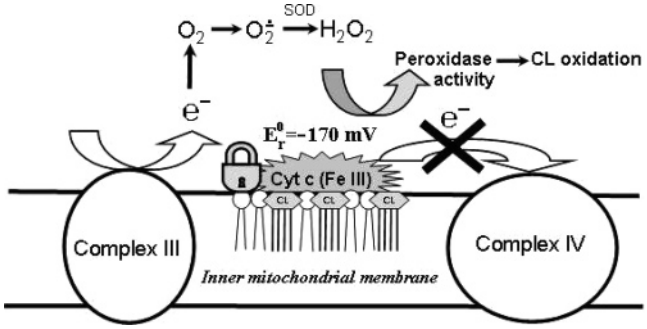

Scheme 2: Thermodynamic Cycle of Reduction and Unfolding of Cyt *c* in the Presence of CL

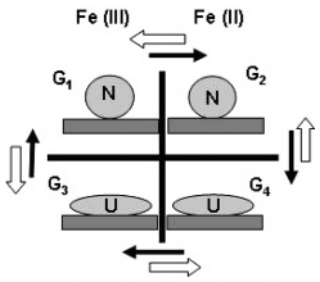

organization of the electron transport chain into integrated respiratory supercomplexes by "gluing together" individual respiratory complexes (*53*, *54*). A part of the intermembrane cyt *c* pool is embedded into respiratory chain supercomplexes (*55*). Our results suggest that CL-bound cyt *c* is not a component of respiratory supercomplexes. Moreover, it is possible that excess CL and its interaction with cyt *c*, as it happens during apoptosis, prevent the correct assembly of respiratory complexes. Mechanisms and specific participants driving redistribution of CL in apoptosis are still poorly characterized although mitochondrial translocation and activity of tBid, a truncated form of a cytosolic protein Bid, seem to be associated with the apoptotic transmembrane migration of CL (*56*−*58*).

The reduction of cyt *c* in mitochondria may be accomplished not only directly via Complex III but also by superoxide anion radicals generated as a result of univalent reduction of molecular oxygen by mitochondrial protein complexes (*3*, *4*). We demonstrated that superoxide cannot effectively reduce CL/cyt *c* complexes. Thus CL/cyt *c* complexes are neither directly reduced by Complex III nor indirectly reduced by $O_2^{\cdot-}$. This suggests that cyt *c*/CL complexes are excluded from electron transport in mitochondria and are likely present in their oxidized form, increasing the probability of the formation of peroxidase Compounds I and II in the presence of oxidizing equivalents such as H_2O_2 or organic and lipid hydroperoxides.

The redox environment of mitochondria is significantly affected by the presence and reactions of ascorbate as a potent reductant localized in mitochondria (*59*). However, ascorbate-driven reduction of cyt *c* to its ferrous form would be inhibitory to the peroxidase reactions of cyt *c* realized within CL/cyt *c* complexes (see below). Our demonstration that CL/cyt *c* complexes are not readily reducible by ascorbate further supports our hypothesis that association with CL acts as a switch turning off normal electron donor−acceptor functions of cyt *c* and facilitating its peroxidase function.

Overall, interactions of cyt *c* with CL during apoptosis represent an essential part of a well-coordinated mechanism of programmed cell death (see Scheme 1). A marked negative shift of the cyt *c* redox potential by CL favors the accumulation of ferri-cyt *c* which is essential for effective peroxidase catalysis. Moreover, the negative redox potential of cyt *c*/CL complexes excludes them from the electron transport chain, causing the disruption of electron flow and facilitating generation of superoxide radicals. Dismutation of the latter yields H_2O_2 that feeds the peroxidase function of cyt *c*/CL complexes.

The Redox State of Cyt c/CL Complexes and Their Peroxidase Function. Inhibition of cyt *c* reduction is important for its peroxidase function, particularly during apoptosis, for several reasons. Peroxidase reactions utilize oxidizing equivalents of H_2O_2 and/or organic (lipid) hydroperoxides to generate potent oxidizing oxo-ferryl intermediates from ferri-cyt *c* [Fe(III)], in which a highly oxidized state of Fe(IV) is active in producing catalytically competent protein-derived (often tyrosyl) radicals (*60*, *61*). The negative shift of the cyt *c* redox potential associated with CL-induced protein structural changes implies that the reduced cyt *c* is much more resistant to denaturation by anionic lipids than the oxidized cyt *c* in line with previous reports (*16*, *62*). Indeed, consideration of a thermodynamic cycle, depicted in Scheme 2, for cyt *c* bound to CL membranes electrostatically (the native tertiary structure) or hydrophopically (partially denatured protein) in the two redox states shows that the free energy of the conversion of cyt *c* into a denatured form is much more positive in the reduced state than in the oxidized state:

$$\Delta G_{red}^{denat} - \Delta G_{ox}^{denat} = (G_4 - G_2) - (G_3 - G_1) = (G_4 - G_3) - (G_2 - G_1) = e(E_N^0 - E_{denat}^0) \approx 9 \text{ kcal/mol} \quad (1)$$

In Scheme 2, G_1 is the free energy of oxidized cyt *c* in the native conformation, G_2 is the free energy of reduced cyt *c* in the native conformation, G_3 is the free energy of the oxidized cyt *c* denatured by the lipid, and G_4 is the free energy of the reduced cyt *c* denatured by the lipid. The thermodynamic cycle (Scheme 2) and eq 1 show direct thermodynamic connection between the difference of free energies of unfolding of cyt *c* in the reduced and oxidized states ($\Delta G_{red}^{denat} = G_4 - G_2$ and $\Delta G_{ox}^{denat} = G_3 - G_1$) and the difference of redox potentials of cyt *c* in the native and denatured conformational states [$E_N^0 = -(G_2 - G_1)/e$ and $E_{denat}^0 = -(G_4 - G_3)/e$]. The predicted difference of stabilities of cyt *c* in the reduced and oxidized states (~9 kcal/mol ≈ 15 kT) is very large, suggesting that the reduced cyt *c* interacting with anionic lipid will be almost entirely in the native-like conformational state.

The denaturing of cyt *c* upon its oxidation and subsequent refolding to a native-like tertiary structure upon reduction, observed in our voltammetry experiments, results in a very large separation of oxidation and reduction peaks for cyt *c* interacting with CL. The peroxidase activity of cyt *c* is

associated with a destabilization of the protein tertiary structure. Thus, the reduced cyt *c* is much less likely to convert into a peroxidase than the oxidized cyt *c*. Factors affecting the redox state of cyt *c* should influence its peroxidase activity and may change the development of apoptosis. For example, increased production of NO•, known to block Complex IV function and increase the concentration of reduced cyt *c* (*59*, *63*), will likely inhibit the peroxidase function of CL/cyt *c* complexes. Along with direct interactions of NO• with reactive intermediates of CL/cyt *c* during peroxidase catalysis (*61*) this may represent an important antioxidant and antiapoptotic mechanism. Moreover, a reducing redox environment for mitochondria (e.g., during hypoxic or ischemic conditions) is also counterproductive for the peroxidase function whereas reoxygenation and reoxidation of cyt *c* is likely to favor its conversion into a catalytically active peroxidase. Not surprisingly, reoxygenation, rather than hypoxia/ischemia, is associated with increased apoptotic damage (*64*).

Finally, while CL binds cyt *c* with a very high affinity, it is not unique as a modifier of cyt *c*'s redox behavior. Other anionic phospholipids, particularly PS, can also confer peroxidase activity on the protein although less effectively than CL (*13*). Studies in this and other laboratories characterized unfolding of the protein upon its binding with CL. Further studies are necessary to detail specific mechanisms through which these conformational rearrangements, particularly in the heme binding site, translate into changes of cyt *c* redox potential and electrochemistry.

REFERENCES

1. Mathews, C. K., van Holde, K. E., and Ahem, K. G. (1999) *Biochemistry*, 3rd ed., Addison Wesley Longman, San Francisco.
2. Pettigrew, G. W., and Moore, G. R. (1987) *Cytochrome c—Biological Aspects*, Springer-Verlag, Berlin and Heidelberg.
3. Pereverzev, M. O., Vygodina, T. V., Konstantinov, A. A., and Skulachev, V. P. (2003) Cytochrome *c*, an ideal antioxidant, *Biochem. Soc. Trans. 31*, 1312−1315.
4. Turrens, J. F. (2003) Mitochondrial formation of reactive oxygen species, *J. Physiol. 552*, 335−344.
5. Gogvadze, V., Orrenius, S., and Zhivotovsky, B. (2006) Multiple pathways of cytochrome *c* release from mitochondria in apoptosis, *Biochim. Biophys. Acta 1757*, 639−647.
6. Garrido, C., Galluzzi, L., Brunet, M., Puig, P. E., Didelot, C., and Kroemer, G. (2006) Mechanisms of cytochrome *c* release from mitochondria, *Cell Death Differ. 13*, 1423−1433.
7. Fadeel, B., and Orrenius, S. (2005) Apoptosis: a basic biological phenomenon with wide-ranging implications in human disease, *J. Intern. Med. 258*, 479−517.
8. Kagan, V. E., Tyurin, V. A., Jiang, J., Tyurina, Y. Y., Ritov, V. B., Amoscato, A. A., Osipov, A. N., Belikova, N. A., Kapralov, A. A., Kini, V., Vlasova, I. I., Zhao, Q., Zou, M., Di, P., Svistunenko, D. A., Kurnikov, I. V., and Borisenko, G. G. (2005) Cytochrome *c* acts as a cardiolipin oxygenase required for release of proapoptotic factors, *Nat. Chem. Biol. 1*, 223−232.
9. Yoshida, H., Kawane, K., Koike, M., Mori, Y., Uchiyama, Y., and Nagata, S. (2005) Phosphatidylserine-dependent engulfment by macrophages of nuclei from erythroid precursor cells, *Nature 437*, 754−758.
10. Wang, H., Blair, D. F., Ellis, W. R., Jr., Gray, H. B., and Chan, S. I. (1986) Temperature dependence of the reduction potential of CuA in carbon monoxide inhibited cytochrome *c* oxidase, *Biochemistry 25*, 167−171.
11. Belikova, N. A., Vladimirov, Y. A., Osipov, A. N., Kapralov, A. A., Tyurin, V. A., Potapovich, M. V., Basova, L. V., Peterson, J., Kurnikov, I. V., and Kagan, V. E. (2006) Peroxidase activity and structural transitions of cytochrome *c* bound to cardiolipin-containing membranes, *Biochemistry 45*, 4998−5009.
12. Diederix, R. E., Ubbink, M., and Canters, G. W. (2002) Peroxidase activity as a tool for studying the folding of c-type cytochromes, *Biochemistry 41*, 13067−13077.
13. Kagan, V. E., Borisenko, G. G., Tyurina, Y. Y., Tyurin, V. A., Jiang, J., Potapovich, A. I., Kini, V., Amoscato, A. A., and Fujii, Y. (2004) Oxidative lipidomics of apoptosis: redox catalytic interactions of cytochrome *c* with cardiolipin and phosphatidylserine, *Free Radical Biol. Med. 37*, 1963−1985.
14. Pinheiro, T. J. (1994) The interaction of horse heart cytochrome *c* with phospholipid bilayers. Structural and dynamic effects, *Biochimie 76*, 489−500.
15. Nantes, I. L., Zucchi, M. R., Nascimento, O. R., and Faljoni-Alario, A. (2001) Effect of heme iron valence state on the conformation of cytochrome *c* and its association with membrane interfaces. A CD and EPR investigation, *J. Biol. Chem. 276*, 153−158.
16. Letellier, L., and Shechter, E. (1973) Correlations between structure and spectroscopic properties in membrane model system. Fluorescence and circular dichroism of the cytochrome *c*-cardiolipin system, *Eur. J. Biochem. 40*, 507−512.
17. Pinheiro, T. J., Cheng, H., Seeholzer, S. H., and Roder, H. (2000) Direct evidence for the cooperative unfolding of cytochrome *c* in lipid membranes from H-(2)H exchange kinetics, *J. Mol. Biol. 303*, 617−626.
18. Oellerich, S., Lecomte, S., Paternostre, M., Heimburg, T., and Hildebrandt, P. (2004) Peripheral and integral binding of cytochrome *c* to phospholipids vesicles, *J. Phys. Chem. B 108*, 3871−3878.
19. Brown, L. R., and Wuthrich, K. (1977) NMR and ESR studies of the interactions of cytochrome *c* with mixed cardiolipin-phosphatidylcholine vesicles, *Biochim. Biophys. Acta 468*, 389−410.
20. Soussi, B., Bylund-Fellenius, A. C., Schersten, T., and Angstrom, J. (1990) ^{1}H-n.m.r. evaluation of the ferricytochrome *c*-cardiolipin interaction. Effect of superoxide radicals, *Biochem. J. 265*, 227−232.
21. Domanov, Y. A., Molotkovsky, J. G., and Gorbenko, G. P. (2005) Coverage-dependent changes of cytochrome *c* transverse location in phospholipid membranes revealed by FRET, *Biochim. Biophys. Acta 1716*, 49−58.
22. Salamon, Z., and Tollin, G. (1997) Interaction of horse heart cytochrome *c* with lipid bilayer membranes: effects on redox potentials, *J. Bioenerg. Biomembr. 29*, 211−221.
23. Jing, W. G., Liu, C. W., Tang, J. L., Wu, Z. Y., Dong, S. J., and Wang, E. K. (2003) Electrochemical and spectroscopic study on the interaction of cytochrome *c* with anionic lipid vesicles, *Chin. J. Chem. 21*, 544−549.
24. Wackerbarth, H., and Hildebrandt, P. (2003) Redox and conformational equilibria and dynamics of cytochrome *c* at high electric fields, *ChemPhysChem. 4*, 714−724.
25. Petrovic, J., Clark, R. A., Yue, H., Waldeck, D. H., and Bowden, E. F. (2005) Impact of surface immobilization and solution ionic strength on the formal potential of immobilized cytochrome *c*, *Langmuir 21*, 6308−6316.
26. Tyurina, Y. Y., Kini, V., Tyurin, V. A., Vlasova, I. I., Jiang, J., Kapralov, A. A., Belikova, N. A., Yalowich, J. C., Kurnikov, I. V., and Kagan, V. E. (2006) Mechanisms of cardiolipin oxidation by cytochrome *c*: relevance to pro- and antiapoptotic functions of etoposide, *Mol. Pharmacol. 70*, 706−717.
27. Zahn, J. A., Arciero, D. M., Hooper, A. B., Coats, J. R., and DiSpirito, A. A. (1997) Cytochrome *c* peroxidase from *Methylococcus capsulatus* Bath, *Arch. Microbiol. 168*, 362−372.
28. Gudz, T. I., Tserng, K. Y., and Hoppel, C. L. (1997) Direct inhibition of mitochondrial respiratory chain complex III by cell-permeable ceramide, *J. Biol. Chem. 272*, 24154−24158.
29. Thierbach, G., and Reichenbach, H. (1981) Myxothiazol, a new inhibitor of the cytochrome *b-c*1 segment of the respiratory chain, *Biochim. Biophys. Acta 638*, 282−289.
30. Birch-Machin, M. A., Briggs, H. L., Saborido, A. A., Bindoff, L. A., and Turnbull, D. M. (1994) An evaluation of the measurement of the activities of complexes I-IV in the respiratory chain of human skeletal muscle mitochondria, *Biochem. Med. Metab. Biol. 51*, 35−42.
31. Ritov, V. B., Menshikova, E. V., and Kelley, D. E. (2004) High-performance liquid chromatography-based methods of enzymatic analysis: electron transport chain activity in mitochondria from human skeletal muscle, *Anal. Biochem. 333*, 27−38.
32. Ragan, C. I., Wilson, M. T., Darley-Usmar, V., and Lowe, P. N. (1987) in *Mitochondria: A Practical Approach* (Darley-Usmar, V., Rickwood, D., and Wilson, M. T., Eds.) pp 79−112, IRL Press, Oxford.

33. Yonetani T. (1966) in *Biochemical Preparations* (Maehly, A. C., Ed.) pp 11, 14−20, John Wiley & Sons, New York.
34. McCord, J. M., and Fridovich, I. (1968) The reduction of cytochrome *c* by milk xanthine oxidase, *J. Biol. Chem. 243*, 5753−5760.
35. Heineman, W. R., Meckstroth, M. L., Norris, B. J., and Su, C.-Ho. (1979) Optically transparent thin layer electrode techniques for the study of biological redox systems, *J. Electroanal. Chem. 104*, 577−585.
36. Wei, J., Liu, H., Dick, A. R., Yamamoto, H., He, Y., and Waldeck, D. H. (2002) Direct wiring of cytochrome *c*'s heme unit to an electrode: electrochemical studies, *J. Am. Chem. Soc. 124*, 9591−9599.
37. Fedurco, M., Augustynski, J., Indiani, C., Smulevich, G., Antalik, M., Bano, M., Sedlak, E., Glascock, M. C., and Dawson, J. H. (2005) Electrochemistry of unfolded cytochrome *c* in neutral and acidic urea solutions, *J. Am. Chem. Soc. 127*, 7638−7646.
38. Yue, H., Waldeck, D. H., Petrovic, J., and Clark, R. A. (2006) The effect of ionic strength on the electron-transfer rate of surface immobilized cytochrome *c*, *J. Phys. Chem. B 110*, 5062−5072.
39. Napper, A. M., Liu, H., and Waldeck, D. H. (2001) The nature of electronic coupling between ferrocene and gold through alkanethiolate monolayers on electrodes: the importance of chain composition, interchain coupling, and quantum interference, *J. Phys. Chem. B 105*, 7699−7707.
40. Feng, Z. Q., Imabayashi, Sh., Kakiuchi, T., and Niki, K. (1997) Long-range electron-transfer reaction rates to cytochrome *c* across long- and short-chain alkanethiol self-assembled monolayers: Electroreflectance studies, *J. Chem. Soc., Faraday Trans. 93*, 1367−1370.
41. Lide, D., Ed. (1994/95) *Handbook of Chemistry and Physics*, 75th ed., p 965, CRC Press, Cleveland, OH.
42. Sagun, K. C., Carcamo, J. M., and Golde, D. W. (2005) Vitamin C enters mitochondria via facilitative glucose transporter 1 (Glut1) and confers mitochondrial protection against oxidative injury, *FASEB J. 19*, 1657−1667.
43. Myer, Y. P., and Kumar, S. (1984) Ascorbate reduction of horse heart cytochrome *c*. A zero-energy reduction reaction, *J. Biol. Chem. 259*, 8144−8150.
44. Petlicki, J., and van de Ven, T. G. M. (1998) The equilibrium between the oxidation of hydrogen peroxide by oxygen and the dismutation of peroxyl or superoxide radicals in aqueous solutions in contact with oxygen, *J. Chem. Soc., Faraday Trans. 94*, 2763−2767.
45. Butler, J., Koppenol, W. H., and Margoliash, E. (1982) Kinetics and mechanism of the reduction of ferricytochrome c by the superoxide anion, *J. Biol. Chem. 257*, 10747−10750.
46. Birch-Machin, M. A., and Turnbull, D. M. (2001) Assaying mitochondrial respiratory complex activity in mitochondria isolated from human cells and tissues, *Methods Cell Biol. 65*, 97−117.
47. Kalyanaraman, B., Perez-Reyes, E., and Mason, R. P. (1979) The reduction of nitroso-spin traps in chemical and biological systems, a cautionary note, *Tetrahedron Lett. 50*, 4809−4812.
48. Kennedy, Ch. H., Pryor, W. A., Winston, G. W., and Church, D. F. (1986) Hydroperoxide-induced radical production in liver mitochondria, *Biochem. Biophys. Res. Commun. 141*, 1123−1129.
49. Chen, Y. R., and Mason, R. P. (2002) Mechanism in the reaction of cytochrome *c* oxidase with organic hydroperoxides: an ESR spin-trapping investigation, *Biochem. J. 365*, 461−469.
50. Petrosillo, G., Ruggiero, F. M., and Pistolese, M. (2004) Paradies G. Ca^{2+}-induced reactive oxygen species production promotes cytochrome *c* release from rat liver mitochondria via mitochondrial permeability transition (MPT)-dependent and MPT-independent mechanisms: role of cardiolipin, *J. Biol. Chem. 279*, 53103−53108.
51. Crouser, E. D., Gadd, M. E., Julian, M. W., Huff, J. E., Broekemeier, K. M., Robbins, K. A., and Pfeiffer, D. R. (2003) Quantitation of cytochrome *c* release from rat liver mitochondria, *Anal. Biochem. 317*, 67−75.
52. Fernandez, M. G., Troiano, L., Moretti, L., Nasi, M., Pinti, M., Salvioli, S., Dobrucki, J., and Cossarizza, A. (2002) Early changes in intramitochondrial cardiolipin distribution during apoptosis, *Cell Growth Differ. 13*, 449−455.
53. Zhang, M., Mileykovskaya, E., and Dowhan, W. (2005) Cardiolipin is essential for organization of complexes III and IV into a supercomplex in intact yeast mitochondria, *J. Biol. Chem. 280*, 29403−29408.
54. Zhang, M., Mileykovskaya, E., and Dowhan, W. (2002) Gluing the respiratory chain together. Cardiolipin is required for supercomplex formation in the inner mitochondrial membrane, *J. Biol. Chem. 277*, 43553−43556.
55. Bianchi, C., Genova, M. L., Parenti, Castelli, G., and Lenaz, G. (2004) The mitochondrial respiratory chain is partially organized in a supercomplex assembly: kinetic evidence using flux control analysis, *J. Biol. Chem. 279*, 36562−36569.
56. Kuwana, T., Mackey, M. R., Perkins, G., Ellisman, M. H., Latterich, H., Schneiter, R., Green, D. R., and Newmeyer, D. D. (2002) Bid, Bax, and lipids cooperate to form supramolecular openings in the outer mitochondrial membrane, *Cell 111*, 331−342.
57. Epand, R. F., Martinou, J.-C., Montessuit, S., and Epand, R. M. (2003) Transbilayer lipid diffusion promoted by Bax: implications for apoptosis, *Biochemistry 42*, 14576−14582
58. Tyurin, V. A., Tyurina, Y. Y., Osipov, A. N., Belikova, N. A., Basova, L. V., Kapralov, A. A., Bayir, H., and Kagan, V. E. Interactions of lyso-cardiolipins with cytochrome *c* and tBid: conflict or assistance in apoptosis (2006) *Cell Death Differ.* (ahead of print).
59. Heck, D. E., Kagan, V. E., Shvedova, A. A., and Laskin, J. D. (2005) An epigrammatic (abridged) recounting of the myriad tales of astonishing deeds and dire consequences pertaining to nitric oxide and reactive oxygen species in mitochondria with an ancillary missive concerning the origins of apoptosis, *Toxicology 208*, 259−271.
60. Chen, Y. R., Chen, C. L., Chen, W., Zweier, J. L., Augusto, O., Radi, R., and Mason, R. P. (2004) Formation of protein tyrosine ortho-semiquinone radical and nitrotyrosine from cytochrome *c*-derived tyrosyl radical, *J. Biol. Chem. 279*, 18054−18062.
61. Vlasova, I. I., Tyurin, V. A., Kapralov, A. A., Kurnikov, I. V., Osipov, A. N., Potapovich, M. V., Stoyanovsky, D. A., and Kagan, V. E. (2006) Nitric oxide inhibits peroxidase activity of cytochrome *c*·cardiolipin complex and blocks cardiolipin oxidation, *J. Biol. Chem. 281*, 14554−14562.
62. Bhuyan, A. K., and Udgaonkar, J. B. (2004) Folding of horse cytochrome *c* in the reduced state, *J. Mol. Biol. 312*, 1135−1160.
63. Brunori, M., Giuffre, A., Forte, E., Mastronicola, D., Barone, M. C., and Sarti, P. (2004) Control of cytochrome *c* oxidase activity by nitric oxide, *Biochim. Biophys. Acta 1655*, 365−371.
64. Du, G., Mouithys-Mickalad, A., and Sluse, F. E. (1998) Generation of superoxide anion by mitochondria and impairment of their functions during anoxia and reoxygenation in vitro, *Free Radical Biol. Med. 25*, 1066−1074.

BI061854K